

Crystallization, structural study and analysis of intermolecular interactions of a 2-aminobenzoxazole–fumaric acid molecular salt

Surayyo Razzoqova,^a Batirbay Torambetov,^{a*} Matluba Amanova,^b Shakhnoza Kadirova,^a Aziz Ibragimov^b and Jamshid Ashurov^c

Received 24 October 2022

Accepted 21 November 2022

Edited by J. Reibenspies, Texas A & M University, USA

Keywords: 2-aminobenzoxazole; fumaric acid; co-crystal; salt; molecular and crystal structure; Hirshfeld surface analysis; pairwise interaction energy.

CCDC reference: 2221183

Supporting information: this article has supporting information at journals.iucr.org/e

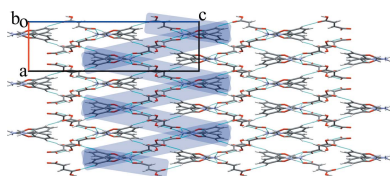
^aNational University of Uzbekistan named after Mirzo Ulugbek, 4 University St, Tashkent, 100174, Uzbekistan, ^bInstitute of General and Inorganic Chemistry, Academy of Sciences of Uzbekistan, 100170, M. Ulugbek Str 77a, Tashkent, Uzbekistan, and ^cInstitute of Bioorganic Chemistry, Academy of Sciences of Uzbekistan, M. Ulugbek, Str. 83, Tashkent, 700125, Uzbekistan. *Correspondence e-mail: torambetov_b@mail.ru

The new organic salt, 2-aminobenzoxazol-3-ium 3-carboxyprop-2-enoate, $C_7H_7N_2O^+ \cdot C_4H_3O_4^-$, of the two bioactive compounds 2-aminobenzoxazole and fumaric acid, crystallizes in the orthorhombic space group *Pbca* using classical evaporation of their solution in water. The usual topological analysis revealed four classical (N–H···O and O–H···O) and two non-classical (C–H···O) hydrogen bonds in the structure. Stacking was found as well for a pair of 2-aminobenzoxazolium cations. A Hirshfeld surface analysis including the two-dimensional fingerprint plots was performed to define the residual π – π interactions and to quantify the influences of different types of interactions by means of topological analysis. Analysis of the pairwise interaction energies was used to prove the formation of the corrugated paired layers of cation–anion dimers parallel to the plane (001) as a basic structural motif in the topological, as well as in the energetic structure of the crystal. It showed that the layers are connected by the hydrogen bonds inside and by stacking and π – π interactions and general dispersion between them.

1. Chemical context

Benzoxazole derivatives are important heterocyclic compounds that exhibit a broad range of biological activities, including antibacterial (Paramashivappa *et al.*, 2003), antimicrobial (Erol *et al.*, 2022), antitumor (Imaizumi *et al.*, 2020), anti-inflammatory (Parlapalli *et al.*, 2017), analgesic (Ali *et al.*, 2022; Sattar *et al.*, 2020), antitubercular (Šlachtová *et al.*, 2018), herbicidal (Sangi *et al.*, 2019) and fungicidal (Fan *et al.*, 2022). 2-Aminobenzoxazoles have been found to act as ligands for the internal ribosome entry site (IRES) RNA of the hepatitis C virus (HCV) (Rynearson *et al.*, 2014).

The formation of a salt or co-crystal presents a useful tool for advantageously modifying the physicochemical properties of an active pharmaceutical ingredient (*e.g.* bioavailability and processing characteristics) without altering its basic chemical structure and pharmacological properties (Guillory *et al.*, 2003; Callear *et al.*, 2009). The pharmaceutical co-crystal can be explained as a multi-component crystal in which at least one of the molecular components is an API, along with the other component called the co-crystal former (Soares *et al.*, 2014). The co-crystal former is believed to help the active drug to disintegrate into small particles and to be transported to the blood stream where the drug is intended to play its role, and

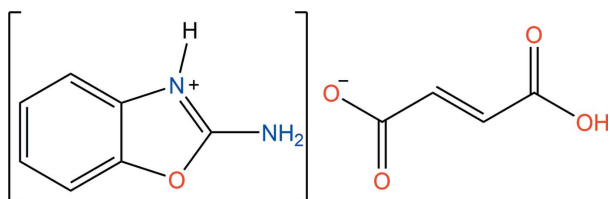


OPEN ACCESS

Published under a CC BY 4.0 licence

still protect the product's stability so that it has the greatest benefits and effectiveness (Blagden *et al.*, 2007). It has been reported that the co-crystallization process allowed the binding of two or more crystal components in a single crystalline lattice *via* hydrogen bonding and van der Waals intermolecular interactions without breaking the bonds or making new covalent bonds (Sonawane *et al.*, 2013; Sheikh *et al.*, 2009).

The organic acids containing the donor and acceptor groups capable of classical hydrogen bonding are used for multi-component assembly, so they are frequently chosen as building blocks in supramolecular crystal engineering (Xu *et al.*, 2019). Fumaric acid is the *E*-isomer of butenedioic acid and is one of the organic compounds found widely in nature. Fumaric acid is also a key intermediate in the biosynthesis of organic acids, and forms interesting one-, two- and three-dimensional supramolecular architectures as adducts with various amines (Franklin *et al.*, 2009; Batchelor *et al.*, 2000).



Herein, we report on the crystal structure and Hirshfeld surface analysis of a new co-crystal of the 2-aminobenzoxazole–fumaric acid molecular salt (2ABHF).

2. Structural commentary

The co-crystal salt of 2-aminobenzoxazole and fumaric acid crystallizes in the primitive centrosymmetric orthorhombic space group *Pbca*. As seen in Fig. 1, the asymmetric unit of 2ABHF consists of a 2-aminobenzoxazolium cation and a semifumarate anion.

Atom N1 in the 2-aminobenzoxazolium cation is protonated. The 2-aminobenzoxazole ring of 2ABHF is essentially planar, with a maximum deviations from the general planarity

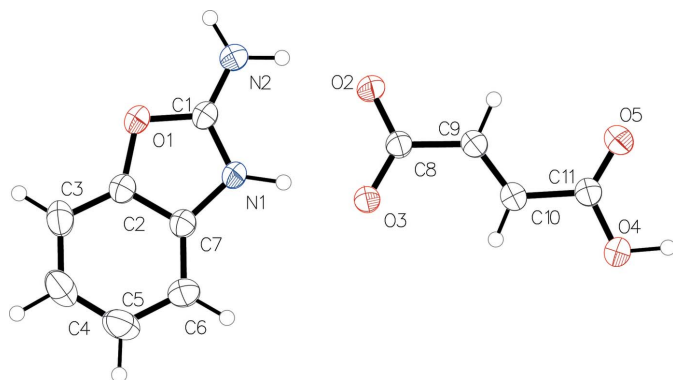


Figure 1

Molecular structure of the title compound. Displacement ellipsoids are shown at the 50% probability level.

Table 1

Hydrogen-bond geometry (Å, °).

<i>D</i> –H··· <i>A</i>	<i>D</i> –H	H··· <i>A</i>	<i>D</i> ··· <i>A</i>	<i>D</i> –H··· <i>A</i>
C6–H6···O1 ⁱ	0.93	2.58	3.4929 (17)	167
C3–H3···O5 ⁱⁱ	0.93	2.51	3.2563 (17)	137
N1–H1···O3	0.99 (2)	1.69 (2)	2.6720 (14)	175.8 (17)
O4–H4A···O2 ⁱⁱⁱ	1.00 (2)	1.60 (2)	2.5913 (14)	174 (2)
N2–H2A···O3 ^{iv}	0.90 (2)	1.94 (2)	2.8355 (16)	176.4 (18)
N2–H2B···O2	0.94 (2)	1.89 (2)	2.7873 (16)	157.8 (18)

Symmetry codes: (i) $-x + \frac{1}{2}, y + \frac{1}{2}, z$; (ii) $-x + \frac{1}{2}, -y + 1, z + \frac{1}{2}$; (iii) $-x + 1, y + \frac{1}{2}, -z + \frac{1}{2}$; (iv) $-x + \frac{1}{2}, y - \frac{1}{2}, z$.

of 0.019 (1) Å for the atom C1. The amino group in the 2-aminobenzoxazolium cation is planar, the sum of bond angles at the N atom being 359.99°.

The semifumarate anion is slightly twisted, showing a deviation from planarity of 0.175 (1) Å for atom O2 and a dihedral angle between the carboxylate (O2/O3/C8) and carboxylic acid (O4/O5/C10) mean planes of 15.6 (2)°.

3. Supramolecular features

Regarding the van der Waals radii proposed in Bondi (1964) for all the atoms except hydrogen (Rowland & Taylor, 1996), four classical hydrogen bonds of two types are found in the crystal structure (Table 1). The first type is N–H···O. It is the most obvious interaction type, forming a dimer comprising an aminobenzoxazolium cation and a semifumarate anion in their original positions (x, y, z) with the bonds N1–H1···O3 and N2–H2B···O2. The other N–H···O hydrogen bond, N2–H2A···O3, connects the aminobenzoxazolium cation with its neighbouring semifumarate anion (the symmetry operation is $\frac{1}{2} - x, -\frac{1}{2} + y, z$). As seen in Fig. 2, this, together with a hydrogen bond of the second type (O–H···O), leads to the formation of layers of dimers along the (001) plane. This O4–H4A···O2 hydrogen bond connects two semifumarate anions (original and its symmetry equivalent $1 - x, \frac{1}{2} + y, \frac{1}{2} - z$). The components within a layer are connected by hydrogen bonds, while stacking/ π – π interactions or general dispersion connect the layers with each other (Fig. 3). Seemingly, the stacking is formed between the original aminobenzoxazolium cation and its symmetry equivalent at $-x, 1 - y, 1 - z$, because the

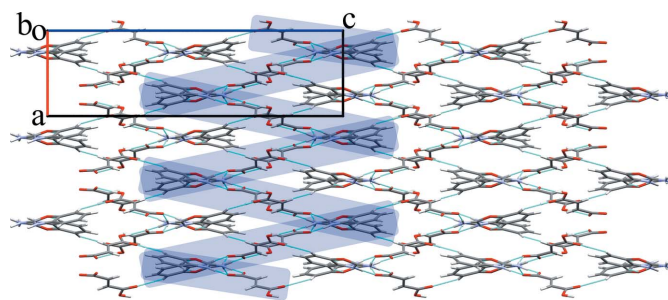
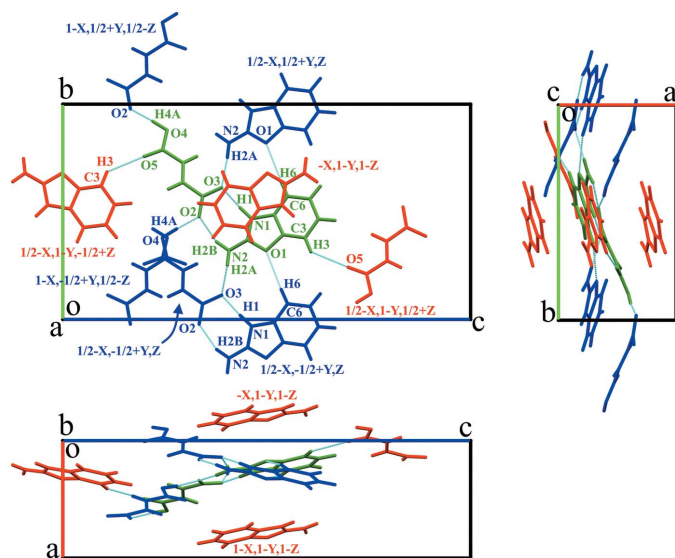


Figure 2

Crystal packing of the corrugated layers parallel to the (001) plane with the hydrogen bonds in cyan. Projection in the [010] direction.

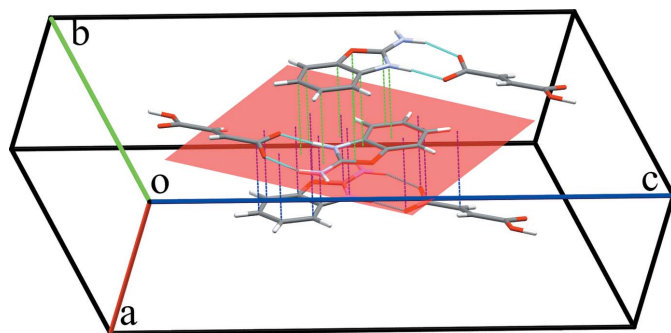

Figure 3

Crystal packing of the molecules from the same (in blue) and adjacent (in red) layers connected to the initial dimer (in green) with specific interactions. The colour codes of the atoms participating in interactions and corresponding symmetry operations of neighbours are similar.

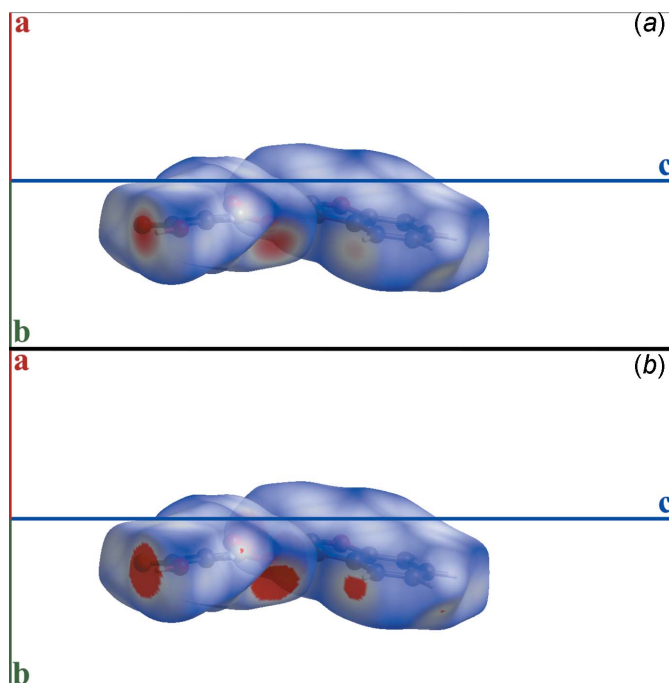
distance between the mean planes of the benzoxazolium fragments is 3.469 (2) Å (Fig. 4). In addition, there are two weak non-classical C—H...O hydrogen bonds in the structure. One of them stabilizes the layers by binding the dimers along the [010] direction together with the classical hydrogen bond N2—H2A...O3. The other one is its counterpart stabilizing the interlayer interactions.

4. Hirshfeld surface analysis

To further investigate the intermolecular interactions present in the title compound, a Hirshfeld surface analysis (Spackman & Byrom, 1997) was performed, and the two-dimensional fingerprint plots were generated with *CrystalExplorer17* (Spackman *et al.*, 2021). The Hirshfeld surface with the


Figure 4

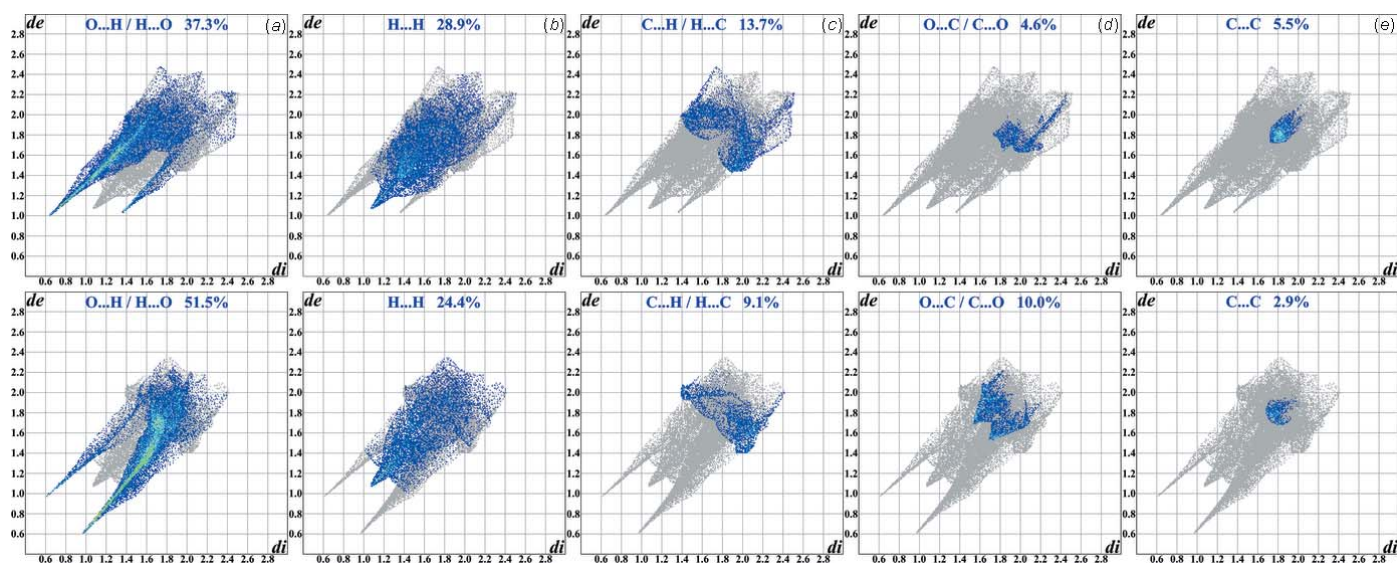
The molecular stacking (green projections on the 2-aminobenzoxazolium mean plane) and π - π interactions (blue projections) formed between adjacent dimers.


Figure 5

Distribution of d_{norm} on the Hirshfeld surfaces of the cation and anion with the default normalization (a) and renormalized (b).

normalized contact distance (d_{norm}) mapped over it was built using standard 'high' resolution. It is shown in Fig. 5 in two variants: (a) with the default scaling (−0.7348, 1.1456 Å for the aminobenzoxazolium cation and −0.7771, 1.1324 Å for semifumarate anion) and (b) showing the minimal shortening in van der Waals radii (the lower limit of d_{norm} renormalized to −0.0001 Å). However, some interactions are obviously overestimated, such as H...H (small red dots on the renormalized Hirshfeld surfaces). This is caused by the use of van der Waals radii by Bondi with a markedly overestimated radius for hydrogen atoms (Rowland & Taylor, 1996). Indeed, the biggest shortening occurs for the classical hydrogen bonds, but it is seen that all the donor and acceptor sites are involved in non-covalent interactions obeying Eters' rules (Eter, 1990; Bernstein *et al.*, 1995).

The two-dimensional (2D) fingerprint plots (Spackman & McKinnon, 2002) are shown in Fig. 6. The most significant interactions whose contribution into the Hirshfeld surface area exceeds 5.0% at least for one of the ions in the structure are O...H/H...O (37.3 and 51.5% for the aminobenzoxazolium and semifumarate moieties, respectively), H...H (28.9 and 24.4%), C...H/H...C (13.7 and 9.1%), O...C/C...O (4.6 and 10.0%) and finally C...C (5.5 and 2.9%). Considering such a shortening of the intermolecular distances, hydrogen bonding can be considered the most important type of interaction in the structure. However, π - π interactions are also present to a large extent, which is easy to see from the localization of O...C/C...O and C...C contacts around the carbon atoms of the aromatic system of the cation and carboxylate moiety of the anion (Fig. 7). The interactions


Figure 6

Contributions of the contacts O...H/H...O (a), H...H (b), C...H/H...C (c), O...C/C...O (d) and C...C (e) to the two-dimensional fingerprint plots built using the Hirshfeld surfaces of the cation (at the top) and anion (at the bottom).

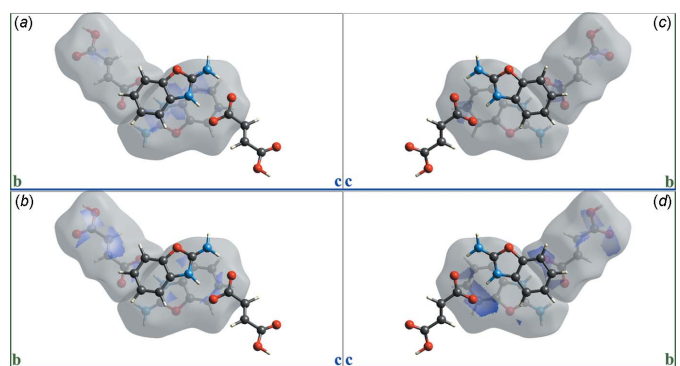
between the original aminobenzoxazolium cation with its symmetry equivalent at $1-x, 1-y, 1-z$ as well as the same symmetry equivalent of the semifumarate anion are of particular interest. They are difficult to recognize from the structural data without additional processing using the Hirshfeld surface analysis but can play an important role in the interlayer binding. It should be mentioned that the sharp peaks in the fingerprint plots reaching values less than the van der Waals radii of the corresponding atom types whose appearance is usually associated with the appearance of intermolecular interactions are seen only for some of all the aforementioned interactions. They are O...H/H...O, H...H and C...C for both moieties and O...C/C...O for the semifumarate anion.

5. Analysis of the pairwise interaction energies

The interactions and the structural motifs in the crystal were assumed from the previous topological analysis and the next step is to confirm the supposed model using the approach of pairwise interactions in crystals (Konovalova *et al.*, 2010; Shishkin *et al.*, 2012). This approach allows the energetic structure of a crystal to be defined. A two-step procedure was used for the current structure. In the first step, the individual ions were considered as the building units and the hydrogen-bonded dimer of the initial ions was found to be the most strongly bound fragment of the crystal structure. It was therefore taken as a building unit for the second step, and all the following calculations were repeated from scratch. The approach was used in the same way as proposed in Shishkin *et al.* (2012), so just the general options concerning the calculations are shown below. The functional used was B97 (Becke, 1997; Schmider & Becke, 1998) with the parameterized three-body (D3) dispersion correction (Grimme *et al.*, 2010) and

Becke–Johnson dumping (Grimme *et al.*, 2011). The double-zeta basis set augmented with diffuse functions (Dunning, 1989; Kendall & Dunning, 1992; Woon & Dunning, 1993; Peterson *et al.*, 1994; Wilson *et al.*, 1996; Davidson, 1996) was used since the structure contains atoms up to the second period. The conductor-like polarizable continuum model (CPCM) was applied to all the pairs of building units to treat the charged system correctly (Barone & Cossi, 1998). In addition, the Boys–Bernardi counterpoise scheme (Boys & Bernardi, 1970) was also used for the basis set superposition error (BSSE) in the software ORCA 5.0.2 (Neese *et al.*, 2020). The calculations were finalized by building the vector energy diagrams in a standard way (Shishkin *et al.*, 2012).

The interaction in the hydrogen-bonded dimer is about twice as strong as any other interaction between the individual ions ($-24.0 \text{ kcal mol}^{-1}$). This fact allowed us to consider the energetic structure of the crystal using the hydrogen-bonded


Figure 7

The localization of the short contacts C...C (a, c) and O...C/C...O (b, d) onto the Hirshfeld surfaces between the initial hydrogen-bonded dimer and its symmetry equivalents $-x, 1-y, 1-z$ (a, b) and $1-x, 1-y, 1-z$ (c, d).

Table 2

 Symmetry codes, binding types and interaction energies (kcal mol⁻¹) of the building units (dimers) with neighbours.

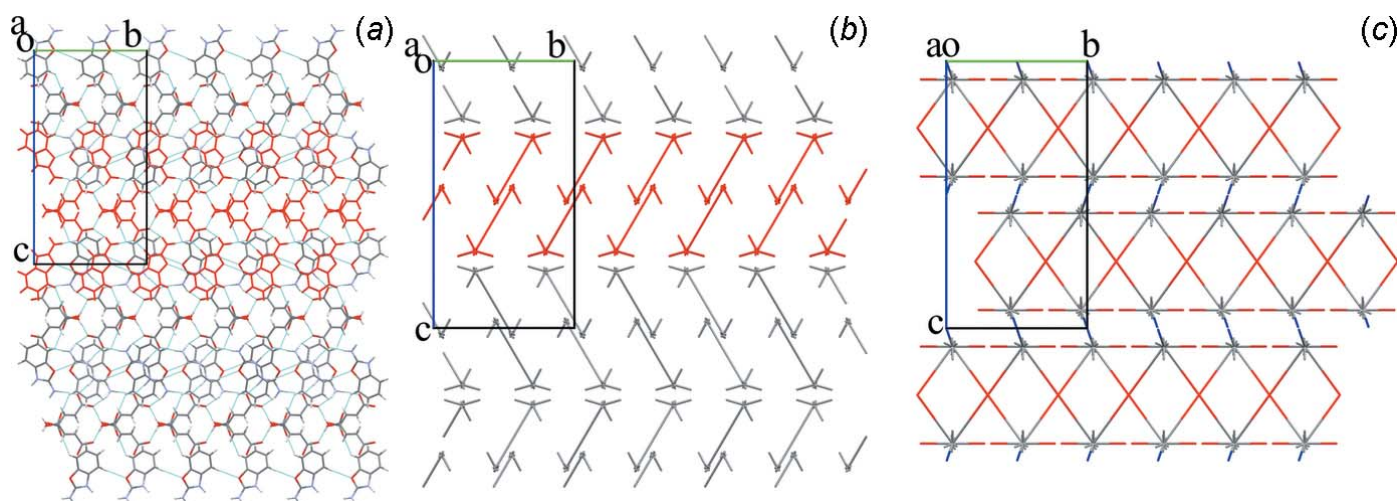
Pair of building units	Symmetry operation of neighbouring building unit	E_{int}	Interaction
1	$-\frac{1}{2} + x, \frac{1}{2} - y, 1 - z$	-2.1	Non-specific
2	$-\frac{1}{2} + x, \frac{3}{2} - y, 1 - z$	-1.6	Non-specific
3	$-x, 1 - y, 1 - z$	-10.6	Stacking
4	$-\frac{1}{2} + x, y, \frac{1}{2} - z$	-3.0	Non-specific
5	$\frac{1}{2} + x, \frac{1}{2} - y, 1 - z$	-2.1	Non-specific
6	$\frac{1}{2} - x, 1 - y, -\frac{1}{2} + z$	-1.4	C3—H3...O5
7	$x, \frac{3}{2} - y, -\frac{1}{2} + z$	-0.9	Non-specific
8	$\frac{1}{2} - x, 1 - y, 1/2 + z$	-1.4	C3—H3...O5
9	$1 - x, -\frac{1}{2} + y, \frac{1}{2} - z$	-11.4	O4—H4A...O2
10	$\frac{1}{2} + x, \frac{3}{2} - y, 1 - z$	-1.6	Non-specific
11	$1 - x, 1 - y, 1 - z$	-10.0	Stacking
12	$\frac{1}{2} + x, y, \frac{1}{2} - z$	-3.0	Non-specific
13	$x, \frac{3}{2} - y, \frac{1}{2} + z$	-0.9	Non-specific
14	$\frac{1}{2} - x, -\frac{1}{2} + y, z$	-10.3	N2—H2A...O3, C6—H6...O1
15	$1 - x, \frac{1}{2} + y, \frac{1}{2} - z$	-11.4	O4—H4A...O2
16	$\frac{1}{2} - x, \frac{1}{2} + y, z$	-10.3	N2—H2A...O3, C6—H6...O1

dimer of the aminobenzoxazolium cation and semifumarate anion as a building unit in all of the following calculations. However, the dimer shows an almost isotropic distribution of interaction energy and just taking into account the types of interactions found during the previous steps allowed us to classify this structure as layered with the corrugated paired layers as a structural motif. The sum of interaction energies between the central dimer and its sixteen neighbours from the first coordination shell is -82.0 kcal mol⁻¹. There are six interactions with energies close to each other and about 3–3.5 times higher than any other in the structure (Table 2). All of the strong in-layer interactions (Fig. 8 in red) correspond to the classical hydrogen bonds or a classical hydrogen bond reinforced by the non-classical hydrogen bond C6—H6...O1. Two residual high energies belong to the aforementioned interlayer stacking and π - π interactions (Fig. 8 in blue). The final non-classical hydrogen bond, C3—H3...O5, introduces a negligible contribution to the interaction of the layers (-1.4 kcal mol⁻¹). The total interaction energies are -51.7

within the layers (001) and -30.3 kcal mol⁻¹ between the layers.

6. Database survey

A search of the Cambridge Structural Database (CSD, Version 5.43, update of November 2021; Groom *et al.*, 2016) for the 2-aminobenzoxazole unit resulted in twelve hits. They include the following analogues: a 5-chloro derivative and its monohydrate and co-crystals with some acids (PAHBW, Lynch, 2004; XUVFAG, Lynch, 2009; XEGLAW, Lynch *et al.*, 2000a; RADGAF, Lynch *et al.*, 2003; LOMTIQ, LOMTEM, LOMTAI, Lynch *et al.*, 2000b; FAFNIL, FAFNEH, Kruszynski *et al.*, 2010), and containing derivatives of the 2-aminobenzoxazole unit (EBAMAY, Coleman *et al.*, 2014; KAVFOC, Colegate *et al.*, 1989; VAKMUT, Silva *et al.*, 2021). The survey shows that in the structures FAFNIL, FAFNEH, LOMTIQ and XEGLAW, the nitrogen atom of the oxazole ring is protonated by a hydrogen from the acid. However, the


Figure 8

Crystal packing of the molecules with hydrogen bonds in cyan (a) and energy vector diagrams of molecules (b) with a single layer in red, as well as the energy vector diagrams of hydrogen-bonded dimers (c) with the hydrogen-bonding (in layer) interactions in red and stacking/ π - π interactions (between layers) in blue.

Table 3
Experimental details.

Crystal data	
Chemical formula	$C_7H_7N_2O^+ \cdot C_4H_3O_4^-$
M_r	250.21
Crystal system, space group	Orthorhombic, <i>Pbca</i>
Temperature (K)	293
a, b, c (Å)	7.0694 (1), 12.9543 (2), 24.5079 (4)
V (Å ³)	2244.41 (6)
Z	8
Radiation type	Cu $K\alpha$
μ (mm ⁻¹)	1.02
Crystal size (mm)	0.16 × 0.14 × 0.12
Data collection	
Diffractometer	XtaLAB Synergy, Single source at home/near, HyPix3000
Absorption correction	Multi-scan <i>CrysAlis PRO</i> ; Rigaku OD, 2021)
T_{\min} , T_{\max}	0.761, 1.000
No. of measured, independent and observed [$I > 2\sigma(I)$] reflections	7276, 2129, 1871
R_{int}	0.023
$(\sin \theta/\lambda)_{\text{max}}$ (Å ⁻¹)	0.609
Refinement	
$R[F^2 > 2\sigma(F^2)]$, $wR(F^2)$, S	0.035, 0.096, 1.05
No. of reflections	2129
No. of parameters	180
H-atom treatment	H atoms treated by a mixture of independent and constrained refinement
$\Delta\rho_{\text{max}}$, $\Delta\rho_{\text{min}}$ (e Å ⁻³)	0.20, -0.16

Computer programs: *CrysAlis PRO* (Rigaku OD, 2021), *SHELXT2018/2* (Sheldrick, 2015a), *SHELXL2016/6* (Sheldrick, 2015b) and *OLEX2* (Dolomanov et al., 2009).

free 2-aminobenzoxazole and its co-crystals with some adducts are not listed in the database. There are numerous submitted structures for fumaric and maleic acids as an adduct for co-crystals of several compounds. However, no co-crystal complexes containing both 2-aminobenzoxazole derivatives and fumaric acid have been documented in the CSD.

7. Synthesis and crystallization

A 1:1 stoichiometric ratio of 2-aminobenzaxazole (0.134 g, 1.0 mmol) and fumaric acid (0.116 g, 1.0 mmol) was dissolved and mixed well in distilled water (3 ml). The mixture was held at 333 K for 10 minutes under stirring. The solution was allowed to stand at room temperature in a beaker with small holes in the cover for evaporation. After about 3 weeks, rectangular single crystals of the $C_7H_7N_2O \cdot C_4H_3O_4$ co-crystal appeared.

8. Refinement

Crystal data, data collection and structure refinement details are summarized in Table 3. The hydrogen atoms were refined isotropically with a mixed model. Those involved in classical hydrogen bonds were found in difference-Fourier maps and are free from any constraints or restraints. The other hydrogen atoms were positioned geometrically (C–H = 0.93 Å) and refined using a riding model with $U_{\text{iso}}(\text{H}) = 1.2U_{\text{eq}}(\text{C})$.

Acknowledgements

We gratefully acknowledge the help with quantum-chemical calculations from the Department of X-ray Diffraction Studies and Quantum Chemistry (SSI Institute for Single Crystals of the National Academy of Sciences of Ukraine) and would like to thank Dr Yevhenii Vaksler for the criticism and advice on the way to conduct the calculations of the pairwise interaction energies for the charged systems.

References

- Ali, S., Omprakash, P., Tengli, A. K., Mathew, B., Basavaraj, M. V., Parkali, P., Chandan, R. S. & Kumar, A. S. (2022). *Polycyclic Aromat. Compd.* **30**, 1–34.
- Barone, V. & Cossi, M. (1998). *J. Phys. Chem. A*, **102**, 1995–2001.
- Batchelor, E., Klinowski, J. & Jones, W. (2000). *J. Mater. Chem.* **10**, 839–848.
- Becke, A. D. (1997). *J. Chem. Phys.* **107**, 8554–8560.
- Bernstein, J., Davis, R. E., Shimon, L. & Chang, N.-L. (1995). *Angew. Chem. Int. Ed. Engl.* **34**, 1555–1573.
- Blagden, N., de Matas, M., Gavan, P. T. & York, P. (2007). *Adv. Drug Deliv. Rev.* **59**, 617–630.
- Bondi, A. (1964). *J. Phys. Chem.* **68**, 441–451.
- Boys, S. F. & Bernardi, F. (1970). *Mol. Phys.* **19**, 553–566.
- Callear, S. K., Hursthouse, M. B. & Threlfall, T. L. (2009). *CrystEngComm*, **11**, 1609–1614.
- Colegate, S., Dorling, P., Huxtable, C., Shaw, T., Skelton, B., Vogel, P. & White, A. (1989). *Aust. J. Chem.* **42**, 1249–1255.
- Coleman, N., Brown, B. M., Oliván-Viguera, A., Singh, V., Olmstead, M. M., Valero, M. S., Köhler, R. & Wulff, H. (2014). *Mol. Pharmacol.* **86**, 342–357.
- Davidson, E. R. (1996). *Chem. Phys. Lett.* **260**, 514–518.
- Dolomanov, O. V., Bourhis, L. J., Gildea, R. J., Howard, J. A. K. & Puschmann, H. (2009). *J. Appl. Cryst.* **42**, 339–341.
- Dunning, T. H. Jr (1989). *J. Chem. Phys.* **90**, 1007–1023.
- Erol, M., Celik, I., Uzunhisarcikli, E. & Kuyucuklu, G. (2022). *Polycycl. Aromat. Compd.* **42**, 1679–1696.
- Etter, M. C. (1990). *Acc. Chem. Res.* **23**, 120–126.
- Fan, L., Luo, Z., Yang, C., Guo, B., Miao, J., Chen, Y., Tang, L. & Li, Y. (2022). *Mol. Divers.* **26**, 981–992.
- Franklin, S. & Balasubramanian, T. (2009). *Acta Cryst.* **C65**, o58–o61.
- Grimme, S., Antony, J., Ehrlich, S. & Krieg, H. (2010). *J. Chem. Phys.* **132**, 154104.
- Grimme, S., Ehrlich, S. & Goerigk, L. (2011). *J. Comput. Chem.* **32**, 1456–1465.
- Groom, C. R., Bruno, I. J., Lightfoot, M. P. & Ward, S. C. (2016). *Acta Cryst.* **B72**, 171–179.
- Guillory, J. K. (2003). *J. Med. Chem.* **46**, 1277–1277.
- Imaizumi, T., Otsubo, S., Komai, M., Takada, H., Maemoto, M., Kobayashi, A. & Otsubo, N. (2020). *Bioorg. Med. Chem.* **28**, 115622.
- Kendall, R. A., Dunning, T. H. Jr & Harrison, R. J. (1992). *J. Chem. Phys.* **96**, 6796–6806.
- Konovalova, I. S., Shishkina, S. V., Paponov, B. V. & Shishkin, O. V. (2010). *CrystEngComm*, **12**, 909–916.
- Kruszynski, R. & Trzesowska-Kruszynska, A. (2010). *Acta Cryst.* **C66**, o449–o454.
- Lynch, D. E. (2004). *Acta Cryst.* **E60**, o1715–o1716.
- Lynch, D. E. (2009). CSD Communication (refcode XUVFAG, CCDC 716694). CCDC, Cambridge, England.
- Lynch, D. E., Barfield, J., Frost, J., Antrobus, R. & Simmons, J. (2003). *Cryst. Eng.* **6**, 109–122.
- Lynch, D. E., Daly, D. & Parsons, S. (2000a). *Acta Cryst.* **C56**, 1478–1479.
- Lynch, D. E., Singh, M. & Parsons, S. (2000b). *Cryst. Eng.* **3**, 71–79.
- Neese, F., Wennmohs, F., Becker, U. & Riplinger, C. (2020). *J. Chem. Phys.* **152**, 224108.

- Paramashivappa, R., Phani Kumar, P., Subba Rao, P. V. & Srinivasa Rao, A. (2003). *Bioorg. Med. Chem. Lett.* **13**, 657–660.
- Parlapalli, A. & Manda, S. (2017). *J. Chem. Pharm. Res.* **9**(9), 57–62.
- Peterson, K. A., Woon, D. E. & Dunning, T. H. Jr (1994). *J. Chem. Phys.* **100**, 7410–7415.
- Rigaku OD (2021). *CrysAlis PRO*. Rigaku Oxford Diffraction, Yarnton, England.
- Rowland, R. S. & Taylor, R. (1996). *J. Phys. Chem.* **100**, 7384–7391.
- Rynearson, K. D., Charrette, B., Gabriel, C., Moreno, J., Boerneke, M. A., Dibrov, S. M. & Hermann, T. (2014). *Bioorg. Med. Chem. Lett.* **24**, 3521–3525.
- Sangi, D. P., Meira, Y. G., Moreira, N. M., Lopes, T. A., Leite, M. P., Pereira-Flores, M. E. & Alvarenga, E. S. (2019). *Pest Manag. Sci.* **75**, 262–269.
- Sattar, R., Mukhtar, R., Atif, M., Hasnain, M. & Irfan, A. (2020). *J. Heterocycl. Chem.* **57**, 2079–2107.
- Schmider, H. L. & Becke, A. D. (1998). *J. Chem. Phys.* **108**, 9624–9631.
- Sheikh, A. Y., Rahim, S. A., Hammond, R. B. & Roberts, K. J. (2009). *CrystEngComm*, **11**, 501–509.
- Sheldrick, G. M. (2015a). *Acta Cryst.* **A71**, 3–8.
- Sheldrick, G. M. (2015b). *Acta Cryst.* **C71**, 3–8.
- Shishkin, O. V., Dyakonenko, V. V. & Maleev, A. V. (2012). *CrystEngComm*, **14**, 1795–1804.
- Silva, L. A., Hottes, E., da Silva, A. M., Freire, L. M. S., Guedes, G. P. & Ferreira, A. B. B. (2021). *J. Braz. Chem. Soc.* **32**, 1009–1016.
- Šlachťová, V. & Brulíková, L. (2018). *ChemistrySelect* **3**, 4653–4662.
- Soares, F. L. F. & Carneiro, R. L. (2014). *J. Pharm. Biomed. Anal.* **89**, 166–175.
- Sonawane, A. R., Rawat, S. S. & Janolkar, N. N. (2013). *Asian J. Biomed. Pharm. Sci.* **27**, 1–8.
- Spackman, M. A. & Byrom, P. G. (1997). *Chem. Phys. Lett.* **267**, 215–220.
- Spackman, M. A. & McKinnon, J. J. (2002). *CrystEngComm*, **4**, 378–392.
- Spackman, P. R., Turner, M. J., McKinnon, J. J., Wolff, S. K., Grimwood, D. J., Jayatilaka, D. & Spackman, M. A. (2021). *J. Appl. Cryst.* **54**, 1006–1011.
- Wilson, A. K., van Mourik, T. & Dunning, T. H. Jr (1996). *J. Mol. Struct. Theochem*, **388**, 339–349.
- Woon, D. E. & Dunning, T. H. Jr (1993). *J. Chem. Phys.* **98**, 1358–1371.
- Xu, W., Lu, Y., Xia, Y., Liu, B., Jin, S., Zhong, B., Wang, D. & Guo, M. (2019). *J. Mol. Struct.* **1189**, 81–93.

supporting information

Acta Cryst. (2022). E78, 1277-1283 [https://doi.org/10.1107/S2056989022011185]

Crystallization, structural study and analysis of intermolecular interactions of a 2-aminobenzoxazole–fumaric acid molecular salt

Surayyo Razzoqova, Batirbay Torambetov, Matluba Amanova, Shakhnoza Kadirova, Aziz Ibragimov and Jamshid Ashurov

Computing details

Data collection: *CrysAlis PRO* (Rigaku OD, 2021); cell refinement: *CrysAlis PRO* (Rigaku OD, 2021); data reduction: *CrysAlis PRO* (Rigaku OD, 2021); program(s) used to solve structure: *SHELXT2018/2* (Sheldrick, 2015a); program(s) used to refine structure: *SHELXL2016/6* (Sheldrick, 2015b); molecular graphics: Olex2 (Dolomanov *et al.*, 2009); software used to prepare material for publication: Olex2 (Dolomanov *et al.*, 2009).

2-Aminobenzoxazol-3-ium 3-carboxyprop-2-enoate

Crystal data

$C_7H_7N_2O^+ \cdot C_4H_3O_4^-$

$M_r = 250.21$

Orthorhombic, *Pbca*

$a = 7.0694$ (1) Å

$b = 12.9543$ (2) Å

$c = 24.5079$ (4) Å

$V = 2244.41$ (6) Å³

$Z = 8$

$F(000) = 1040$

$D_x = 1.481$ Mg m⁻³

Cu *Kα* radiation, $\lambda = 1.54184$ Å

Cell parameters from 4322 reflections

$\theta = 3.6$ – 70.5°

$\mu = 1.02$ mm⁻¹

$T = 293$ K

Needle, clear light colourless

$0.16 \times 0.14 \times 0.12$ mm

Data collection

XtaLAB Synergy, Single source at home/near,

HyPix3000

diffractometer

Radiation source: micro-focus sealed X-ray

tube, PhotonJet (Cu) X-ray Source

Detector resolution: 10.0000 pixels mm⁻¹

ω scans

Absorption correction: multi-scan

CrysAlisPro; Rigaku OD, 2021)

$T_{\min} = 0.761$, $T_{\max} = 1.000$

7276 measured reflections

2129 independent reflections

1871 reflections with $I > 2\sigma(I)$

$R_{\text{int}} = 0.023$

$\theta_{\max} = 70.0^\circ$, $\theta_{\min} = 3.6^\circ$

$h = -8 \rightarrow 7$

$k = -9 \rightarrow 15$

$l = -29 \rightarrow 25$

Refinement

Refinement on F^2

Least-squares matrix: full

$R[F^2 > 2\sigma(F^2)] = 0.035$

$wR(F^2) = 0.096$

$S = 1.05$

2129 reflections

180 parameters

0 restraints

Primary atom site location: structure-invariant direct methods

Hydrogen site location: mixed

H atoms treated by a mixture of independent and constrained refinement

$w = 1/[\sigma^2(F_o^2) + (0.0485P)^2 + 0.5023P]$

where $P = (F_o^2 + 2F_c^2)/3$

$(\Delta/\sigma)_{\max} < 0.001$

$$\Delta\rho_{\max} = 0.20 \text{ e } \text{\AA}^{-3}$$

$$\Delta\rho_{\min} = -0.16 \text{ e } \text{\AA}^{-3}$$

Extinction correction: *SHELXL2016/6*
(Sheldrick 2015b),
 $\text{Fc}^* = k\text{Fc}[1 + 0.001x\text{Fc}^2\lambda^3/\sin(2\theta)]^{-1/4}$
Extinction coefficient: 0.00154 (19)

Special details

Geometry. All esds (except the esd in the dihedral angle between two l.s. planes) are estimated using the full covariance matrix. The cell esds are taken into account individually in the estimation of esds in distances, angles and torsion angles; correlations between esds in cell parameters are only used when they are defined by crystal symmetry. An approximate (isotropic) treatment of cell esds is used for estimating esds involving l.s. planes.

Fractional atomic coordinates and isotropic or equivalent isotropic displacement parameters (\AA^2)

	<i>x</i>	<i>y</i>	<i>z</i>	$U_{\text{iso}}^*/U_{\text{eq}}$
O1	0.17549 (16)	0.32002 (7)	0.49841 (4)	0.0404 (3)
O3	0.35863 (16)	0.61279 (7)	0.38952 (4)	0.0403 (3)
O2	0.33909 (18)	0.47799 (7)	0.33433 (4)	0.0483 (3)
O4	0.59585 (19)	0.87984 (7)	0.25587 (4)	0.0499 (3)
O5	0.49429 (19)	0.75736 (8)	0.19951 (4)	0.0533 (3)
N1	0.26884 (18)	0.46854 (8)	0.46302 (5)	0.0350 (3)
N2	0.2529 (2)	0.32025 (9)	0.40757 (5)	0.0473 (3)
C7	0.23633 (19)	0.48645 (10)	0.51866 (5)	0.0334 (3)
C8	0.3664 (2)	0.57206 (9)	0.34298 (5)	0.0345 (3)
C1	0.2335 (2)	0.36996 (10)	0.45327 (5)	0.0352 (3)
C2	0.1779 (2)	0.39363 (10)	0.54042 (6)	0.0358 (3)
C11	0.5249 (2)	0.78833 (10)	0.24496 (5)	0.0365 (3)
C10	0.4884 (2)	0.72758 (10)	0.29520 (5)	0.0395 (3)
H10	0.523490	0.755361	0.328689	0.047*
C9	0.4091 (2)	0.63688 (10)	0.29419 (5)	0.0398 (3)
H9	0.376287	0.610288	0.260234	0.048*
C6	0.2553 (2)	0.57237 (11)	0.55113 (6)	0.0427 (4)
H6	0.294549	0.635506	0.537043	0.051*
C3	0.1326 (2)	0.37945 (12)	0.59423 (6)	0.0465 (4)
H3	0.092064	0.316219	0.607875	0.056*
C5	0.2129 (2)	0.55992 (13)	0.60616 (7)	0.0509 (4)
H5	0.225909	0.615872	0.629634	0.061*
C4	0.1516 (3)	0.46617 (13)	0.62683 (6)	0.0524 (4)
H4	0.122296	0.461317	0.663738	0.063*
H1	0.305 (3)	0.5194 (15)	0.4348 (8)	0.064 (6)*
H4A	0.613 (3)	0.9197 (18)	0.2214 (9)	0.091 (7)*
H2A	0.219 (3)	0.2538 (16)	0.4034 (8)	0.059 (5)*
H2B	0.294 (3)	0.3593 (16)	0.3773 (8)	0.070 (6)*

Atomic displacement parameters (\AA^2)

	U^{11}	U^{22}	U^{33}	U^{12}	U^{13}	U^{23}
O1	0.0619 (6)	0.0247 (5)	0.0345 (5)	-0.0050 (4)	0.0037 (4)	0.0047 (4)
O3	0.0674 (7)	0.0250 (5)	0.0287 (5)	-0.0012 (4)	0.0088 (4)	-0.0011 (4)
O2	0.0852 (8)	0.0237 (5)	0.0359 (5)	-0.0046 (5)	0.0142 (5)	-0.0037 (4)

O4	0.0817 (9)	0.0348 (5)	0.0332 (5)	-0.0152 (5)	0.0041 (5)	0.0024 (4)
O5	0.0897 (9)	0.0405 (6)	0.0296 (5)	-0.0093 (6)	-0.0004 (5)	-0.0009 (4)
N1	0.0524 (7)	0.0227 (5)	0.0300 (6)	-0.0019 (5)	0.0053 (5)	0.0025 (4)
N2	0.0812 (10)	0.0263 (6)	0.0343 (7)	-0.0064 (6)	0.0067 (6)	-0.0021 (5)
C7	0.0412 (7)	0.0286 (6)	0.0305 (7)	0.0016 (5)	0.0014 (6)	0.0023 (5)
C8	0.0480 (8)	0.0251 (6)	0.0305 (7)	0.0028 (5)	0.0064 (6)	0.0000 (5)
C1	0.0482 (8)	0.0254 (6)	0.0320 (7)	-0.0008 (5)	0.0016 (6)	0.0032 (5)
C2	0.0448 (7)	0.0298 (7)	0.0327 (7)	0.0001 (6)	0.0008 (6)	0.0028 (5)
C11	0.0482 (8)	0.0313 (6)	0.0299 (7)	-0.0007 (6)	0.0033 (6)	0.0007 (5)
C10	0.0562 (9)	0.0355 (7)	0.0268 (7)	-0.0066 (6)	0.0029 (6)	0.0002 (5)
C9	0.0628 (9)	0.0304 (7)	0.0264 (6)	-0.0021 (6)	0.0019 (6)	-0.0006 (5)
C6	0.0558 (9)	0.0304 (7)	0.0419 (8)	0.0017 (6)	0.0014 (7)	-0.0037 (6)
C3	0.0575 (9)	0.0467 (8)	0.0354 (8)	-0.0010 (7)	0.0044 (7)	0.0105 (6)
C5	0.0630 (10)	0.0488 (9)	0.0408 (8)	0.0083 (8)	-0.0001 (7)	-0.0130 (7)
C4	0.0636 (10)	0.0635 (10)	0.0303 (7)	0.0083 (8)	0.0046 (7)	0.0001 (7)

Geometric parameters (Å, °)

O1—C1	1.3456 (16)	C7—C6	1.375 (2)
O1—C2	1.4034 (16)	C8—C9	1.4918 (18)
O3—C8	1.2580 (15)	C2—C3	1.370 (2)
O2—C8	1.2519 (16)	C11—C10	1.4839 (17)
O4—C11	1.3148 (17)	C10—H10	0.9300
O4—H4A	1.00 (2)	C10—C9	1.302 (2)
O5—C11	1.2035 (16)	C9—H9	0.9300
N1—C7	1.4022 (17)	C6—H6	0.9300
N1—C1	1.3231 (17)	C6—C5	1.391 (2)
N1—H1	0.99 (2)	C3—H3	0.9300
N2—C1	1.2991 (18)	C3—C4	1.385 (2)
N2—H2A	0.90 (2)	C5—H5	0.9300
N2—H2B	0.94 (2)	C5—C4	1.385 (2)
C7—C2	1.3785 (19)	C4—H4	0.9300
C1—O1—C2	105.82 (10)	O5—C11—O4	123.88 (12)
C11—O4—H4A	109.9 (13)	O5—C11—C10	124.05 (13)
C7—N1—H1	127.8 (11)	C11—C10—H10	118.7
C1—N1—C7	107.72 (11)	C9—C10—C11	122.53 (13)
C1—N1—H1	124.4 (11)	C9—C10—H10	118.7
C1—N2—H2A	123.0 (12)	C8—C9—H9	117.3
C1—N2—H2B	116.4 (12)	C10—C9—C8	125.44 (13)
H2A—N2—H2B	120.4 (17)	C10—C9—H9	117.3
C2—C7—N1	106.32 (11)	C7—C6—H6	121.8
C6—C7—N1	132.90 (13)	C7—C6—C5	116.49 (14)
C6—C7—C2	120.77 (13)	C5—C6—H6	121.8
O3—C8—C9	119.97 (11)	C2—C3—H3	122.5
O2—C8—O3	123.71 (12)	C2—C3—C4	115.09 (14)
O2—C8—C9	116.32 (11)	C4—C3—H3	122.5
N1—C1—O1	111.91 (11)	C6—C5—H5	119.2

N2—C1—O1	120.18 (12)	C4—C5—C6	121.59 (14)
N2—C1—N1	127.90 (13)	C4—C5—H5	119.2
C7—C2—O1	108.22 (11)	C3—C4—C5	122.02 (14)
C3—C2—O1	127.76 (13)	C3—C4—H4	119.0
C3—C2—C7	124.02 (14)	C5—C4—H4	119.0
O4—C11—C10	112.07 (11)		
O1—C2—C3—C4	178.81 (15)	C1—O1—C2—C7	0.54 (15)
O3—C8—C9—C10	19.2 (2)	C1—O1—C2—C3	-179.11 (15)
O2—C8—C9—C10	-161.08 (16)	C1—N1—C7—C2	-0.81 (16)
O4—C11—C10—C9	176.32 (15)	C1—N1—C7—C6	177.88 (16)
O5—C11—C10—C9	-4.1 (3)	C2—O1—C1—N1	-1.09 (16)
N1—C7—C2—O1	0.15 (15)	C2—O1—C1—N2	177.33 (14)
N1—C7—C2—C3	179.82 (14)	C2—C7—C6—C5	0.0 (2)
N1—C7—C6—C5	-178.51 (15)	C2—C3—C4—C5	-0.3 (3)
C7—N1—C1—O1	1.21 (17)	C11—C10—C9—C8	-179.35 (14)
C7—N1—C1—N2	-177.07 (15)	C6—C7—C2—O1	-178.73 (13)
C7—C2—C3—C4	-0.8 (2)	C6—C7—C2—C3	0.9 (2)
C7—C6—C5—C4	-1.1 (2)	C6—C5—C4—C3	1.2 (3)

Hydrogen-bond geometry (Å, °)

<i>D</i> —H... <i>A</i>	<i>D</i> —H	H... <i>A</i>	<i>D</i> ... <i>A</i>	<i>D</i> —H... <i>A</i>
C6—H6...O1 ⁱ	0.93	2.58	3.4929 (17)	167
C3—H3...O5 ⁱⁱ	0.93	2.51	3.2563 (17)	137
N1—H1...O3	0.99 (2)	1.69 (2)	2.6720 (14)	175.8 (17)
O4—H4A...O2 ⁱⁱⁱ	1.00 (2)	1.60 (2)	2.5913 (14)	174 (2)
N2—H2A...O3 ^{iv}	0.90 (2)	1.94 (2)	2.8355 (16)	176.4 (18)
N2—H2B...O2	0.94 (2)	1.89 (2)	2.7873 (16)	157.8 (18)

Symmetry codes: (i) $-x+1/2, y+1/2, z$; (ii) $-x+1/2, -y+1, z+1/2$; (iii) $-x+1, y+1/2, -z+1/2$; (iv) $-x+1/2, y-1/2, z$.